CHIN. PHYS. LETT. Vol. 37, No. 9 (2020) 098501

Room-Temperature Processed Amorphous ZnRhCuO Thin Films with p-Type Transistor and Gas-Sensor Behaviors

Bojing Lu(陆波静)[1], Rumin Liu(刘如敏)[1], Siqin Li(李思嵌)[1], Rongkai Lu(吕容恺)[1], Lingxiang Chen(陈凌翔)[2*], Zhizhen Ye(叶志镇)[1,2], and Jianguo Lu(吕建国)[1,2*]

[1]*State Key Laboratory of Silicon Materials, School of Materials Science and Engineering, Zhejiang University, Hangzhou 310027, China*

[2]*Key Laboratory for Biomedical Engineering of Ministry of Education, College of Biomedical Engineering and Instrument Science, Zhejiang University, Hangzhou 310027, China*

(Received 16 May 2020; accepted 15 July 2020; published online 1 September 2020)

We examine an amorphous oxide semiconductor (AOS) of ZnRhCuO. The *a*-ZnRhCuO films are deposited at room temperature, having a high amorphous quality with smooth surface, uniform thickness and evenly distributed elements, as well as a high visible transmittance above 87% with a wide bandgap of 3.12 eV. Using *a*-ZnRhCuO films as active layers, thin-film transistors (TFTs) and gas sensors are fabricated. The TFT behaviors demonstrate the p-type nature of *a*-ZnRhCuO channel, with an on-to-off current ratio of $\sim 1 \times 10^3$ and field-effect mobility of $0.079\,\mathrm{cm^2V^{-1}s^{-1}}$. The behaviors of gas sensors also prove that the *a*-ZnRhCuO films are of p-type conductivity. Our achievements relating to p-type *a*-ZnRhCuO films at room temperature with TFT devices may pave the way to practical applications of AOSs in transparent flexible electronics.

PACS: 85.30.De, 85.30.Tv, 73.61.Jc, 81.05.Gc DOI: 10.1088/0256-307X/37/9/098501

Since Hosono *et al.* reported amorphous InGaZnO thin-film transistors (TFTs) in 2004,[1] amorphous oxide semiconductors (AOSs) have been widely studied, owing to their potential applications in flat panel displays,[2] synapse devices,[3] and sensors.[4] Due to their amorphous nature, AOSs have inherent merits over crystalline semiconductors, with respect to their low-temperature process, uniform deposition, and large-area fabrication. AOSs commonly have a wide band gap, making them transparent in the visible region. Therefore, AOSs play an important role in modern microelectronics, transparent electronics, and flexible wearable devices.

While most of AOSs are of n-type conductivity, such as InZnO,[5] InGaZnO,[1,6] ZnSnO,[7] and ZnAlSnO,[8] the use of p-type AOSs is very limited. It is well known that the realization of p-type conductivity in oxide semiconductors is rather difficult.[9] However, p-type oxides are always necessary for transparent electronics. Complementary metal-oxide semiconductor (CMOS) inverters using p-type and n-type AOS TFTs can greatly reduce energy consumption in the field of information and communication, enabling one to realize novel devices, such as transparent flexible circuits. To date, several p-type oxides have also been reported, including SnO,[10,11] NiO,[12] Cu_2O,[13,14] and $CuAlO_2$,[15] but these are all crystalline. Few p-type AOSs have been reported so far,[16–18] which has created something of a bottleneck in terms of the development of transparent electronics. Therefore, research into p-type AOSs is of great significance and progress in this area is urgently required.

For this purpose, we prepared *a*-ZnRhCuO films by magnetron sputtering at room temperature. TFTs and gas sensors were fabricated using the *a*-ZnRhCuO active layer, from which the p-type conduction of *a*-ZnRhCuO was firmly confirmed. Our work provides clear clues and references for the further development of the p-type AOS and its associated devices.

In our experiment, amorphous ZnRhCuO films were deposited by radio-frequency magnetron sputtering. The ZnRhCuO targets were sintered using high-purity ZnO, Rh_2O_3 and Cu_2O powders with a Zn:Rh:Cu = 2:1:1 atomic ratio. Quartz and Si/SiO_2 wafers were used as substrates. The Si/SiO_2 substrates consist of a layer of heavily doped p-type silicon (0.001–0.009 Ω·cm) and a layer of insulating SiO_2 (300 nm). The ZnRhCuO films were deposited at room temperature for 25 min, in a high-purity oxygen (99.999%) atmosphere (1.5 Pa). No subsequent thermal treatment was carried out on the ZnRhCuO films. The bottom-gate ZnRhCuO TFTs were fabricated on p^{++}-Si/SiO_2 substrates, where the p^{++}-Si and SiO_2 were used as the gate electrode and the dielectric layer, respectively. Having deposited the chan-

Supported by the National Natural Science Foundation of China (Grant No. 51741209), and the Zhejiang Provincial Natural Science Foundation of China (Grant Nos. LR16F040001 and LGG19F040005).

*Corresponding authors. Email: chenlingxiang@zju.edu.cn; lujianguo@zju.edu.cn

© 2020 Chinese Physical Society and IOP Publishing Ltd

nel layer, a 100-nm-thick Au/Ni source and drain electrodes were deposited via electron-beam evaporation, using a mask method. The channel length and width of TFTs measured 300 μm and 1000 μm, respectively.

The structure and morphology of the as-prepared ZnRhCuO films were examined by x-ray diffraction (XRD), field-emission scanning electron microscopy (FESEM), and high-resolution transmission electron microscopy (HRTEM). The composition and distribution of elements in films were measured by energy dispersive x-ray (EDX) spectroscopy, attached to an SEM. Optical transmission of the films was performed using an ultraviolet-visible spectrophotometer. The electrical performance of the TFTs was examined using a semiconductor parameter analyzer. The gas detecting behaviors of the films were investigated under different oxygen pressures.

Figure 1(a) shows the XRD pattern of the as-grown ZnRhCuO film at room temperature. The halo peak appears near 23°, generated by the quartz substrate, due to its close-range ordered and long-range disordered microstructure. There are no other obvious diffraction peaks in the spectrum. Our preliminary conclusions are that the ZnRhCuO film is amorphous. Figure 1(b) shows the surface SEM image of the *a*-ZnRhCuO film, with the inset displaying the cross-sectional image. The *a*-ZnRhCuO film has a dense, flat surface without any obvious cracks or holes, which is beneficial for the fabrication of devices. The thickness of the film is about 53 nm, with good uniformity.

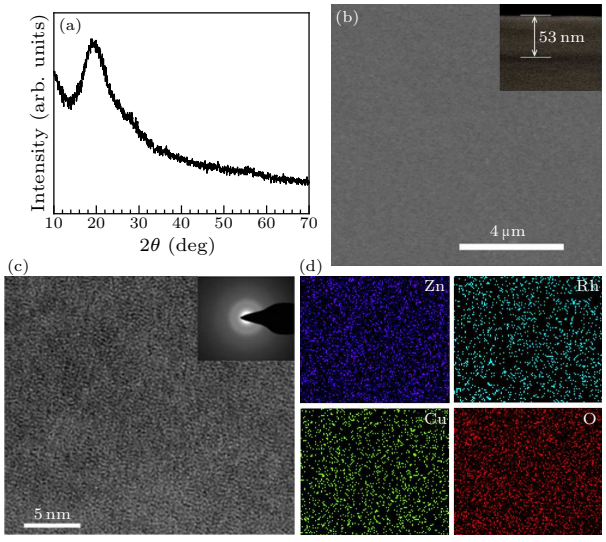

Fig. 1. (a) XRD patterns of *a*-ZnRhCuO thin films deposited on a quartz substrate at room temperature. (b) Surface SEM image of the *a*-ZnRhCuO film, with the inset depicting the cross-sectional profile. (c) HRTEM image of the *a*-ZnRhCuO film, with the inset depicting the corresponding SAED pattern. (d) Element mapping images of Zn, Rh, Cu and O in the *a*-ZnRhCuO film. All samples were grown at room temperature.

To further examine the sample's crystalline property, HRTEM measurements were performed, as shown in Fig. 1(c). There are no obvious lattice structures and no atomic clusters in the ZnRhCuO film. The selected area electron diffraction (SAED) patterns [inset of Fig. 1(c)] display broadly diffused diffraction rings, a typical electron diffraction signature for amorphous materials. The TEM observations provide a firm indication that the as-grown ZnRhCuO film is amorphous in nature. The EDS mappings of the film are shown in Fig. 1(d), revealing the presence of four elements of Zn, Cu, Rh, and O in the film, evenly distributed, and without aggregation or segregation. The determined content in the film is Zn:Rh:Cu = 56:20:24 in atomic ratio, which is in agreement with our target. The uniform distribution of components in the film is necessary and beneficial for reliable device behaviors.

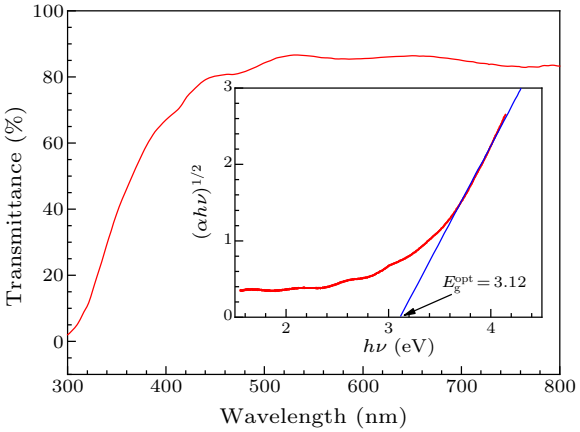

Fig. 2. Optical transmission spectrum of *a*-ZnRhCuO thin film. The inset shows the plot of $(\alpha h\nu)^{1/2} - h\nu$ and linear fit in the ultraviolet region.

Figure 2 depicts the transmission spectrum of the ZnRhCuO films grown at room temperature on quartz substrates. In the visible range, the film has a transmittance above 87%, suggesting that the film is a transparent material. We calculate the optical band gap of the film according to the Tauc equation:[19]

$$\alpha h\nu = C(h\nu - E_g^{opt})^n, \tag{1}$$

where α denotes the absorption coefficient of the film, $h\nu$ represents the photon energy of the incident light, E_g^{opt} is the optical band gap, and the n value represents different electronic transition modes. The amorphous oxide semiconductor is usually an indirect band gap semiconductor; here, n is equal to 2. A linear fit is performed on the ultraviolet region of the $(\alpha h\nu)^{1/2} \sim h\nu$ curve. The horizontal axis intercept is equal to the optical band gap of the amorphous ZnRhCuO film, which is about 3.12 eV, meaning that ZnRhCuO is a wide-band-gap AOS material.

Using the *a*-ZnRhCuO films as active layers, we fabricated TFTs. The inset of Fig. 3(a) shows the schematic structure of *a*-ZnRhCuO TFTs. Figure 3(a) depicts the transfer characteristics of the *a*-ZnRhCuO

TFTs at a drain-source voltage of $V_{DS} = 10$ V. The drain-source current I_{DS} increases in the TFT as the gate-source voltage V_{GS} increases at a negative V_{DS}, clearly indicating the p-type conductivity of the channel. Figure 3(b) shows the output characteristics of the a-ZnRhCuO TFTs. The TFTs display an ohmic contact between the Au/Ni and channel layers, since no evident current crowding is observed at low drain-source voltage. The output curves do not exhibit a clear pinch-off and current saturation. This phenomenon has also been observed in several p-type oxide transistors.[20–23]

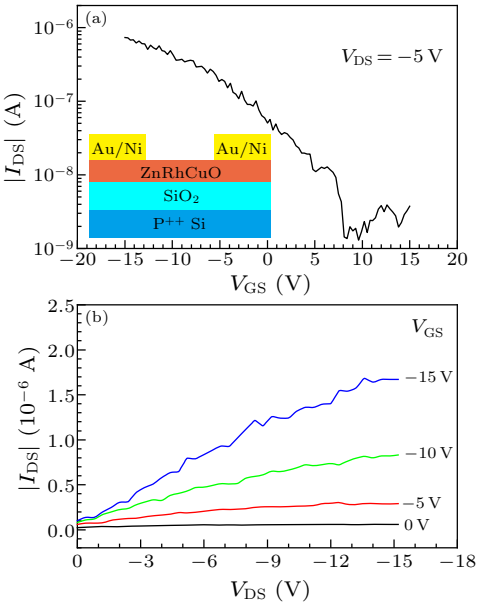

Fig. 3. (a) Transfer characteristics and (b) output characteristics of a-ZnRhCuO TFTs. The inset in (a) shows the schematic structure of the a-ZnRhCuO TFTs.

Based on the transfer curve, the off-state current is in the order of 10^{-9} A, suggesting that there may be a large leakage current in the device. The on-to-off current ratio I_{on}/I_{off} is about $\sim 10^3$, comparable to those previously reported (in the order of 10^2–10^4) for p-type crystalline oxide TFTs.[10–15] The field effect mobility μ_{FE} is calculated by I_{DS}–V_{GS} curves, using the equation:

$$I_{DS}^{1/2} = \sqrt{\frac{W}{2L} C_i \mu_{FE}}\,(V_{GS} - V_{th}), \quad V_{DS} \geqslant V_{GS} - V_{th}, \tag{2}$$

where C_i, W, and L respectively denote the capacitance per unit area of the gate insulator, channel width, and channel length; μ_{FE} is determined to be $0.079\,\mathrm{cm^2V^{-1}s^{-1}}$. Based on previous reports,[10–15] the field-effect mobility of p-type oxide TFTs is rather low, commonly in the range of 0.01–2 $\mathrm{cm^2V^{-1}s^{-1}}$. The μ_{FE} obtained here is a reasonable value, considering that the p-type channel layer is an amorphous oxide.

The electrical transportation of the a-ZnRhCuO film is also investigated with reference to its gas sensing behaviors. Figure 4 illustrates the drain-source current I_{DS} under different oxygen pressures at $V_{DS} = 10$ V, using a TFT device with a gate voltage of 0 V. The I_{DS} value decreases rapidly when the oxygen pressure is evacuated from 10^5 Pa to 100 Pa, and quickly returns to its original value when the oxygen reverts to 10^5 Pa. As derived from the curve, the sensitivity is 2.19, the response time is 19 s, and the recovery time is 32 s. It is believed that this change in the value of I_{DS} results from the desorption and adsorption process of oxygen molecules, a well-known phenomenon in the case of oxide semiconductors.[20] The oxygen molecules adsorbed by the a-ZnRhCuO film surface attract electrons from the film, leading to a decrease in electron density, and an increase in hole density in the film. In our case, I_{DS} decreases with the desorption of oxygen molecules, which further proves that the a-ZnRhCuO film is of p-type conductivity.

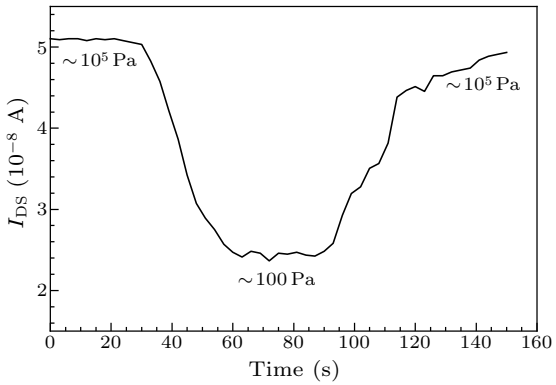

Fig. 4. Temporal current responses of a-ZnRhCuO gas sensors under different oxygen pressures.

In this work, we have developed p-type a-ZnRhCuO films for TFTs and gas sensors. In our case, Zn is the main element; that is to say, the matrix is Zn-rich. In the presence of excessive Zn, the three-dimensional network structure of RhO_6 octahedra and ZnO_4 tetrahedra is still retained in the amorphous state,[16] such that p-type conductivity is possible for AOS.[24] The introduced Cu may further elevate the hole concentration, thereby improving the p-type characteristics, as previously reported in relation to Cu-based p-type oxides.[13–15] To the best of our knowledge, very little research into TFT, using a p-type AOS, has been conducted to date. The progress demonstrated in this work may pave the way not only for the design of logic circuits based on p- and n-type AOSs for transparent electronics, but also for fabricating flexible devices, since the room temperature process is also highly compatible with organic substrates.

In summary, amorphous ZnRhCuO films have been deposited at room temperature and used as

the active layers for TFTs and gas sensors. The *a*-ZnRhCuO films exhibit a rather high amorphous quality, having a high visible transmittance above 87%, with a wide bandgap of 3.12 eV. The *a*-ZnRhCuO TFTs clearly display p-type conductivity in the channel layer, with an on-to-off current ratio of $\sim 1 \times 10^3$, and a field-effect mobility of $0.079\,\mathrm{cm^2V^{-1}s^{-1}}$. The p-type conductivity of *a*-ZnRhCuO films is also confirmed by the fabricated gas sensors. The *a*-ZnRhCuO constitutes a new p-type AOS. The achievement of p-type *a*-ZnRhCuO TFTs and gas sensors, as well as its room-temperature processes, may open the door both to further fundamental research, and to practical applications in terms of transparent and flexible electronics.

References

[1] Nomura K, Ohta H, Takagi A, Kamiya T, Hirano M and Hosono H 2004 *Nature* **432** 488

[2] Wager J F, Yeh B, Hoffman R L and Keszler D A 2014 *Curr. Opin. Solid State Mater. Sci.* **18** 53

[3] Lu B J, Lu Y D, Zhu H J, Zhang J Q, Yue S L, Li S Q, Zhuge F, Ye Z Z and Lu J G 2019 *Mater. Lett.* **249** 169

[4] Jiang Q J, Wu C J, Feng L S, Gong L, Ye Z Z and Lu J G 2015 *Appl. Surf. Sci.* **357** 1536

[5] Yue S L, Lu J G, Lu R K, Li S Q, Lu B J, Zhao Y, Li X F, Zhang J H and Ye Z Z 2019 *IEEE Trans. Electron Devices* **66** 2960

[6] Honda W, Harada S, Ishida S, Arie T, Akita S and Takei K 2015 *Adv. Mater.* **27** 4674

[7] Feng L S, Yu G Y, Li X F, Zhang J H, Ye Z Z and Lu J G 2017 *IEEE Trans. Electron Devices* **64** 206

[8] Jiang Q J, Feng L S, Wu C J, Sun R J, Li X F, Lu B, Ye Z Z and Lu J G 2015 *Appl. Phys. Lett.* **106** 053503

[9] Wang Z W, Nayak P K, Caraveo-Fresca J A S and Alshareef H N 2016 *Adv. Mater.* **28** 3831

[10] Ogo Y, Hiramatsu H, Nomura K, Yanagi H, Kamiya T, Hirano M and Hosono H 2008 *Appl. Phys. Lett.* **93** 032113

[11] Fortunato E, Barros R, Barquinha P, Figueiredo V, Park S, Hwang C and Martins R 2010 *Appl. Phys. Lett.* **97** 052105

[12] Jiang J, Wang X, Zhang Q, Li J and Zhang X X 2013 *Phys. Chem. Chem. Phys.* **15** 6875

[13] Park I J, Jeong C Y, U M, Song S h, Cho I T, Lee J H, Cho E S and Kwon H I 2013 *IEEE Electron Device Lett.* **34** 647

[14] Matsuzaki K, Nomura K, Yanagi H, Kamiya T, Hirano M and Hosono H 2008 *Appl. Phys. Lett.* **93** 202107

[15] Kawazoe H, Yasukawa M, Hyodo H, Kurita M, Yanagi H and Hosono H 1997 *Nature* **389** 939

[16] Kamiya T, Narushima S, Mizoguchi S, Shimizu K, Ueda K, Ohta H, Hirano M and Hosono H 2005 *Adv. Funct. Mater.* **15** 968

[17] Kim S, Cianfrone J A, Sadik P, Kim K W, Ivill M and Norton D P 2010 *J. Appl. Phys.* **107** 103538

[18] Li J, Kaneda T, Tokumitsu E, Koyano M, Mitani T and Shimoda T 2012 *Appl. Phys. Lett.* **101** 052102

[19] Lu J G, Ye Z Z, Huang J Y, Wang L and Zhao B H 2003 *Appl. Surf. Sci.* **207** 295

[20] Yuan G D, Zhang W J, Jie J S, Fan X, Zapien J A, Leung Y H, Luo L B, Wang P F, Lee C S and Lee S T 2008 *Nano Lett.* **8** 2591

[21] Liu W, Xiu F, Sun K, Xie Y, Wang K, Wang Y, Zou J, Yang Z and Liu J 2010 *J. Am. Chem. Soc.* **132** 2498

[22] Lee J, Cha S, Kim J, Nam H, Lee S, Ko W, Wang K, Park J and Hong J 2011 *Adv. Mater.* **23** 4183

[23] Wang F, Seo J, Bayerl D, Shi J, Mi H, Ma Z, Zhao D, Shuai Y, Zhou W and Wang X 2011 *Nanotechnology* **22** 225602

[24] Narushima S, Mizoguchi H, Shimizu K, Ueda K, Ohta H, Hirano M, Kamiya T and Hosono H 2003 *Adv. Mater.* **15** 1409